Geophys. J. Int. (2003) **155,** 213–220

Convective instability of 3-D fluid-saturated geological fault zones heated from below

Chongbin Zhao,[1,2] B. E. Hobbs,[1] H. B. Mühlhaus,[1] A. Ord[1] and Ge Lin[2]

[1]*Predictive Mineral Discovery Coorperative Research Centre, CSIRO Division of Exploration and Mining,* PO Box 1130, *Bentley,* WA 6102, *Australia. E-mail: c.zhao@ned.dem.csiro.au*

[2]*Changsha Institute of Geotectonics, Chinese Academy of Sciences, Changsha, China*

Accepted 2003 May 6. Received 2003 March 17; in original form 2001 December 17

SUMMARY

We conduct a theoretical analysis to investigate the convective instability of 3-D fluid-saturated geological fault zones when they are heated uniformly from below. In particular, we have derived exact analytical solutions for the critical Rayleigh numbers of different convective flow structures. Using these critical Rayleigh numbers, three interesting convective flow structures have been identified in a geological fault zone system. It has been recognized that the critical Rayleigh numbers of the system have a minimum value only for the fault zone of infinite length, in which the corresponding convective flow structure is a 2-D slender-circle flow. However, if the length of the fault zone is finite, the convective flow in the system must be 3-D. Even if the length of the fault zone is infinite, since the minimum critical Rayleigh number for the 2-D slender-circle flow structure is so close to that for the 3-D convective flow structure, the system may have almost the same chance to pick up the 3-D convective flow structures. Also, because the convection modes are so close for the 3-D convective flow structures, the convective flow may evolve into the 3-D finger-like structures, especially for the case of the fault thickness to height ratio approaching zero. This understanding demonstrates the beautiful aspects of the present analytical solution for the convective instability of 3-D geological fault zones, because the present analytical solution is valid for any value of the ratio of the fault height to thickness. Using the present analytical solution, the conditions, under which different convective flow structures may take place, can be easily determined.

Key words: analytical solution, convective instability, critical Rayleigh number, flow structure, geological fault zone.

1 INTRODUCTION

Over the past 5 years, we have been making efforts to develop a practical and predictive tool to explore for giant ore deposits in the upper crust of the Earth. To this end, significant progress has been made towards a better understanding of the basic physical and chemical processes behind ore body formation and mineralization in hydrothermal systems. On the scientific development side, we have developed analytical solutions to answer the following scientific questions (Zhao *et al.* 1998a, 1999a): (1) can the pore-fluid pressure gradient be maintained at the value of the lithostatic pressure gradient in the upper crust of the Earth and (2) can convective pore-fluid flow take place in the upper crust of the Earth if there is a fluid/mass leakage from the mantle to the upper crust of the Earth? On the modelling development side, we have developed numerical methods to model the following problems: (1) convective pore-fluid flow in hydrothermal systems (Zhao *et al.* 1997); (2) coupled reactive pore-fluid flow and multiple species transport in porous media (Zhao *et al.* 1999b); (3) precipitation and dissolution of minerals and rock alteration in the upper crust of the Earth (Zhao *et al.* 1998b); (4) double-diffusion-driven reactive flow transport in deformable fluid-saturated porous media with particular consideration of temperature-dependent chemical reaction rates (Zhao *et al.* 2000a); (5) pore-fluid flow patterns near geological lenses in hydrodynamic and hydrothermal systems (Zhao *et al.* 1999c); (6) dissipative structure of non-equilibrium chemical reactions in fluid-saturated porous media (Zhao *et al.* 2000b); (7) convective pore-fluid flow and the related mineralization in 3-D hydrothermal systems (Zhao *et al.* 2001a); (8) fluid–rock interaction problems associated with the rock alteration and metamorphic process in fluid-saturated hydrothermal/sedimentary basins (Zhao *et al.* 2001b). Note that Rice & Cleary (1976) and McTigue (1986) have also studied the different aspects of this problem. In addition, we have developed numerical methods to model various aspects of the fully coupled problem involving material deformation, pore-fluid flow, heat transfer and species transport/chemical reactions in pore-fluid saturated porous rock masses. The above-mentioned work has significantly enriched our knowledge concerning the physical

and chemical processes related to ore body formation and mineralization in the upper crust of the Earth. However, the convective instability of 3-D geological fault zone systems has not been well studied so far. Since geological fault zones and their surrounding rocks are favourite locations for ore body formation and mineralization to take place, it is important to gain a theoretical insight into convective flow structures in 3-D geological fault zones when they are heated uniformly from below.

The study of convective instability in fluid-saturated porous media was initiated by Horton & Rogers (1945) and Lapwood (1948) approximately half a century ago. Since then, a large number of publications have been produced on this particular research topic. Nield & Bejan (1992) and Phillips (1991) have summarized the related research results in their books. Although the research on the general aspects of the topic is extensive, it is very limited on the convective instability of 3-D geological fault zones when they are heated uniformly from below. In this regard, a geological fault zone is usually represented by a vertically oriented thin finite slab, which is comprised of fluid-saturated porous media. The large and small vertical surfaces of the slab are called the sidewalls and end-walls, respectively. Beck (1972), Zebib & Kassoy (1977) first solved the problem without considering the sidewall heat loss, so their solution is of little value for a vertically oriented geological fault. Considering the sidewall heat loss, Lowell & Shyu (1978) and Murphy (1979) used the Galerkin and simplified methods to obtain the approximate solutions, which may be only used to qualitatively judge some kinds of convective flow structures in the system. To overcome the shortcomings of the approximate solutions presented by Lowell & Shyu (1978) and Murphy (1979), Kassoy & Cotte (1985) used the linear stability approach to produce asymptotic solutions for the above system. Since the asymptotic solutions are only valid when the thickness of the fault approaches zero, it is impossible to use such asymptotic solutions to predict the different critical Rayleigh numbers, under which different convective flow structures, such as the 2-D slender-circle convective flow, the 3-D standard convective flow and the 3-D finger-like convective flow, may occur because the critical Rayleigh numbers of these flows are very close each other, especially for the case where the fault thickness to height ratio is very small. Therefore, there is a definite need for developing exact solutions of the system so that different convective flow structures can be predicted exactly in a 3-D fluid-saturated geological fault zone system. The main purpose of this study is to develop the required exact solutions for different critical Rayleigh numbers, using which different convective flow structures with a similar possibility of occurrence can be accurately identified in the geological fault zone system.

2 GOVERNING EQUATIONS OF THE PROBLEM

For a 3-D fluid-saturated geological fault zone, its thickness is much smaller than both its length and height, as shown in Fig. 1. The fault zone is assumed to be very permeable, compared with its surrounding rocks. The length of the fault may be infinite in the x_1 direction, but we consider the size of convection cells to be H_1 in this direction so that the insolated and impermeable boundary conditions can be added at both $x_1 = 0$ and H_1. In the thickness direction, both the geothermal gradient and hydrostatic pore-fluid pressure gradient are considered and therefore, the geothermal gradient and hydrostatic pore-fluid pressure gradient conditions need to be added at both $x_2 = 0$ and H_2. This means that any perturbation due to temperature within the geological fault zone has little influence on the initial thermal and flow pattern distributions of its surrounding rocks. It is assumed that the fault zone is uniformly heated from below so that the constant temperature and impermeable boundary conditions are added at both $x_3 = 0$ and H_3. In order to facilitate the forthcoming theoretical analysis, the material of the fault zone is assumed to be a homogeneous and isotropic porous medium. If Darcy's law is used to describe pore fluid flow and the Boussinesq approximation is employed to describe a change in pore-fluid density due to a change in pore-fluid temperature, the governing equations of natural convection for an incompressible fluid in a steady state can be expressed as

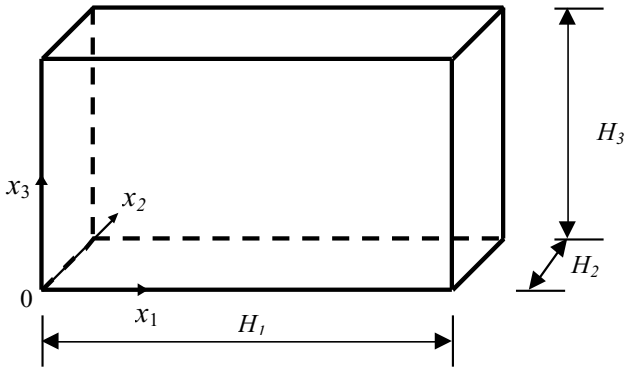

Figure 1. Geometry of the problem.

$$u_{i,i} = 0 \tag{1}$$

$$u_i = \frac{1}{\mu} k_0(-p_{,i} + \rho_f g_i) \tag{2}$$

$$(\rho_0 c_p) u_j T_{,j} = \left(\lambda_0^e T_{,j}\right)_{,j} \tag{3}$$

$$\rho_f = \rho_0[1 - \beta(T - T_0)] \tag{4}$$

$$\lambda_0^e = \phi\lambda_0 + (1 - \phi)\lambda_0^s, \tag{5}$$

where u_i is the Darcy velocity component in the x_i direction; p and T are pressure and temperature; ρ_0 and T_0 are the reference density of the pore fluid and the reference temperature of the medium; μ and c_p are the dynamic viscosity and specific heat of the pore fluid; λ_0 and λ_0^s are the thermal conductivity coefficients for the pore fluid and solid matrix in the porous medium; ϕ and β are the porosity of the medium and the thermal volume expansion coefficient of the pore fluid; k_0 is the permeability of the medium and g_i is the gravity acceleration component in the x_i direction.

The corresponding boundary conditions are as follows:

$$u_1 = 0, \quad T_{,1} = 0 \quad (x_1 = 0 \text{ and } x_1 = H_1) \tag{6}$$

$$p = \rho_0 g_3(H_3 - x_3),$$
$$T = \frac{T_b - T_o}{H_3}(H_3 - x_3) + T_0 \quad (x_2 = 0 \text{ and } x_2 = H_2) \tag{7}$$

$$u_3 = 0, \quad T = T_b \quad (x_3 = 0) \tag{8}$$

$$u_3 = 0, \quad T = T_0 \quad (x_3 = H_3). \tag{9}$$

It is noted that since the perturbed temperature is much smaller than the base temperature on the two vertical surfaces (i.e. $x_2 = 0$ and H_2), it is neglected in eq. (7). However, the effect of this small perturbed temperature due to the convective flow can be offset by using the effective thickness of the fault zone. Generally, the

effective thickness of the fault zone should be a little larger than the physical thickness of the fault zone.

In order to simplify eqs (1)–(3), the following dimensionless variables are defined:

$$x_i^* = \frac{x_i}{H}, \quad T^* = \frac{T - T_0}{\Delta T}, \quad H_i^* = \frac{H_i}{H}$$
$$u_i^* = \frac{H\rho_0 c_p}{\lambda_0^e} u_i, \quad p^* = \frac{k_0 \rho_0 c_p}{\mu \lambda_0^e}(p - p_0), \tag{10}$$

where x_i^* are the dimensionless coordinates; u_i^* is the dimensionless velocity component in the x_i direction; p^* and T^* are the dimensionless pressure and temperature; ΔT is the temperature difference between the bottom and top boundaries of the porous medium; H_1, H_2 and H_3 are the length, thickness and height of the fault zone; H is a reference length; p_0 is the reference static pore-fluid pressure and this reference pressure in the flow domain has a hydrostatic pressure gradient. In the following analysis, H_3 is chosen as the reference length (i.e. $H = H_3$).

Substituting the above dimensionless variables into eqs (1)–(3) yields

$$u_{i,i}^* = 0 \tag{11}$$

$$u_i^* = -p_{,i}^* + Ra\, T^* e_i \tag{12}$$

$$u_j^* T_{,j}^* = T_{,jj}^*, \tag{13}$$

where $\mathbf{e}$ is a unit vector and $\mathbf{e} = e_1\mathbf{i} + e_2\mathbf{j} + e_3\mathbf{k}$ for a general 3-D problem. For the particular problem considered in this study, $e_1 = e_2 = 0$ and $e_3 = 1$ since the acceleration due to gravity is only exerted on the vertical direction. Ra is the Rayleigh number, defined as

$$Ra = \frac{(\rho_0 c_p)\rho_0 g \beta \Delta T k_0 H}{\mu \lambda_0^e}. \tag{14}$$

Using the dimensionless variables, the corresponding boundary conditions can be expressed as

$$u_1^* = 0, \quad T_{,1}^* = 0 \quad \left(x_1^* = 0 \text{ and } x_1^* = H_1^*\right) \tag{15}$$

$$p^* = 0, \quad T^* = 1 - x_3^* \quad \left(x_2^* = 0 \text{ and } x_2^* = H_2^*\right) \tag{16}$$

$$u_3^* = 0, \quad T^* = 1 \quad \left(x_3^\star = 0\right) \tag{17}$$

$$u_3^* = 0, \quad T^* = 0 \quad \left(x_3^* = 1\right). \tag{18}$$

It is noted that the linear stability theory has been used to deal with the convective instability problem in fluid-saturated porous media for many years (Horton & Rogers 1945; Lapwood 1948; Phillips 1991; Nield & Bejan 1992), but there are very seldom analytical solutions to the convective instability problem in 3-D geological zones. Although Kassoy & Cotte (1985) used the linear stability approach to produce asymptotic solutions for the similar problem as stated here, their solutions are only valid when the thickness of the fault zone tends to zero. Therefore, it is desirable to develop exact analytical solutions to this problem so that the onset conditions of the convective flow in the 3-D fault zones can be rigorously investigated.

From the mathematics point of view, the study of the convective instability in the 3-D fault zone is, in essence, to find non-trivial solutions for the partial differential equations expressed in eqs (11)–(13), with the given boundary conditions in eqs (15)–(18). The conditions, under which the non-trivial solutions for the partial differential equations can exist, are the onset conditions of the pore-fluid convective flow in the fault zone, while the non-trivial solutions are the convective flow modes of the fault zone. These onset conditions are often expressed by the related non-dimensional parameters, that is, the critical Rayleigh numbers, of the system. The non-trivial solution corresponding to the minimum critical Rayleigh number is called the fundamental convective flow mode of the system. Bearing this in mind, the conventional linear stability theory is used, in this study, to deal with the convective instability in the 3-D fault zone in a very flexible but logical manner. However, the linear stability analysis is only valid in determining the onset of the convective instability because, once the convective instability occurs, the perturbation approach fails and the non-linear terms in the governing equations cannot be neglected. In this regard, only the most possible triggered convective flow mode of the system is meaningful, if the linear stability theory is used. Since the geometric characteristics of the 3-D fault zone are that the lengths of the fault zone are finite in both the thickness and the height directions (i.e. H_2 and H_3), and that the ratio of fault thickness to height (i.e. H_2/H_3) is very small, the convective flow structure is mainly controlled by the fault height to thickness ratio. As a result, several different convective flow structures may have the same chance of occurring, even if the linear stability theory is used. This means that the linear stability theory can be used to predict several different convective flow structures because the differences in the critical Rayleigh numbers are very small, as will be demonstrated in the next section.

3 ANALYSIS OF CONVECTIVE INSTABILITY OF THE FAULT ZONE SYSTEM

The main purpose in this section is to investigate the condition under which the 3-D convective flow can take place in the fault zone system defined in the previous section. Specifically speaking, the main purpose is to determine the critical Rayleigh number, with which the convective instability of the fault zone system can be examined. From the linear stability theory, the first-order perturbation equations of the hydrothermal system considered here can be expressed as follows:

$$\hat{u}_{i,i}^* = 0 \tag{19}$$

$$\hat{u}_i^* = -\hat{p}_{,i}^* + Ra\, \hat{T}^* e_i \tag{20}$$

$$-\hat{u}_3^* = \hat{T}_{,jj}^*, \tag{21}$$

where $\hat{u}_i^*$ is the dimensionless perturbation velocity components (i.e. dimensionless convective velocity components); $\hat{p}^*$ and $\hat{T}^*$ are the dimensionless perturbation pressure and temperature.

The corresponding boundary conditions for the perturbation variables can be expressed as

$$\hat{u}_1^* = 0, \quad \hat{T}_{,1}^* = 0 \quad \left(x_1^* = 0 \text{ and } x_1^* = H_1^*\right) \tag{22}$$

$$\hat{p}^* = 0, \quad \hat{T}^* = 0 \quad \left(x_2^* = 0 \text{ and } x_2^* = H_2^*\right) \tag{23}$$

$$\hat{u}_3^* = 0, \quad \hat{T}^* = 0 \quad \left(x_3 = 0 \text{ and } x_3^* = 1\right). \tag{24}$$

Inserting eq. (20) into eq. (19) yields the following equation:

$$\hat{p}_{,11}^* + \hat{p}_{,22}^* + \hat{p}_{,33}^* - Ra\hat{T}_{,3}^* = 0. \tag{25}$$

Substituting eq. (20) into eq. (21) yields another equation as follows:

$$\hat{p}_{,3}^* - Ra\hat{T}^* = \hat{T}_{,11}^* + \hat{T}_{,22}^* + \hat{T}_{,33}^*. \tag{26}$$

For the given fault zone configuration shown in Fig. 1, since the lengths of the fault zone in all the three directions are finite, the well-known variable separation method in the mathematics is useful to solve this problem. As we mentioned before, the study of the convective instability in the 3-D fault zone is, in essence, to find

non-trivial solutions for the partial differential equations expressed in eqs (25) and (26), with the prescribed boundary conditions in eqs (22)–(24). The conditions, under which the non-trivial solutions for the partial differential equations can exist, are the onset conditions of the pore-fluid convective flow in the fault zone, and the non-trivial solutions are the convective flow structures of the fault zone. This means that any useful mathematical methods can be used to solve the convective instability problem considered in this study as long as the onset conditions of the pore-fluid convective flow can be found. From the general expression of the derived onset conditions, we need to find the most possible onset condition, which is in correspondence with the minimum critical Rayleigh number of the system in the conventional linear stability analysis sense. For the above reasons, the solutions that satisfy the boundary conditions in the x_1^* and x_2^* directions are expressed as follows:

$$\hat{p}^* = f\left(x_3^*\right)\cos\left(k_1^* x_1^*\right)\sin\left(k_2^* x_2^*\right) \tag{27}$$

$$\hat{T}^* = \theta\left(x_3^*\right)\cos\left(k_1^* x_1^*\right)\sin\left(k_2^* x_2^*\right), \tag{28}$$

where k_1^* and k_2^* are the dimensionless wavenumbers in the x_1^* and x_2^* directions, respectively:

$$k_1^* = \frac{m\pi}{H_1^*} \quad (m = 1, 2, 3, \ldots) \tag{29}$$

$$k_2^* = \frac{n\pi}{H_2^*} \quad (n = 1, 2, 3, \ldots). \tag{30}$$

Using eqs (27) and (28), the boundary conditions in the x_3^* direction can be expressed as

$$Ra\theta\left(x_3^*\right) - f'\left(x_3^*\right) = 0 \quad \left(x_3 = 0 \text{ and } x_3^* = 1\right) \tag{31}$$

$$\theta\left(x_3^*\right) = 0 \quad \left(x_3 = 0 \text{ and } x_3^* = 1\right). \tag{32}$$

Substituting eqs (27) and (28) into eq. (25) yields the following equation:

$$-\left(k_1^{*2} + k_2^{*2}\right) f\left(x_3^*\right) + f''\left(x_3^*\right) - Ra\theta'\left(x_3^*\right) = 0. \tag{33}$$

Inserting eqs (27) and (28) into eq. (26) yields another equation as follows:

$$f'\left(x_3^*\right) = \left(Ra - k_1^{*2} - k_2^{*2}\right)\theta\left(x_3^*\right) + \theta''\left(x_3^*\right). \tag{34}$$

Differentiating eq. (34) with respect to x_3^* twice yields the following equation:

$$f'''\left(x_3^*\right) = \left(Ra - k_1^{*2} - k_2^{*2}\right)\theta''\left(x_3^*\right) + \theta^{(IV)}\left(x_3^*\right). \tag{35}$$

Differentiating eq. (33) with respect to x_3^* once yields another equation as follows:

$$-\left(k_1^{*2} + k_2^{*2}\right) f'\left(x_3^*\right) + f''''\left(x_3^*\right) - Ra\theta''\left(x_3^*\right) = 0. \tag{36}$$

Substituting eqs (34) and (35) into eq. (36) yields the following equation:

$$\theta^{(IV)}\left(x_3^*\right) - 2\left(k_1^{*2} + k_2^{*2}\right)\theta''\left(x_3^*\right) - \left(k_1^{*2} + k_2^{*2}\right)\left(Ra - k_1^{*2} - k_2^{*2}\right)\theta\left(x_3^*\right) = 0. \tag{37}$$

Inserting eq. (34) into eq. (31) yields the boundary conditions depending on θ only:

$$\left(k_1^{*2} + k_2^{*2}\right)\theta\left(x_3^*\right) - \theta''\left(x_3^*\right) = 0 \quad \left(x_3^* = 0 \text{ and } x_3^* = 1\right). \tag{38}$$

The following function satisfies the boundary conditions expressed in eqs (32) and (38):

$$\theta\left(x_3^*\right) = \sin\left(k_3^* x_3^*\right), \tag{39}$$

where k_3^* is the dimensionless wavenumber in the x_3^* direction:

$$k_3^* = q\pi \quad (q = 1, 2, 3, \ldots). \tag{40}$$

Substituting eq. (39) into eq. (37) yields the critical Rayleigh numbers for different convection modes as follows:

$$Ra = \frac{\left(k_1^{*2} + k_2^{*2} + k_3^{*2}\right)^2}{k_1^{*2} + k_2^{*2}}. \tag{41}$$

Substituting the dimensionless wavenumber into eq. (41) yields the following equation:

$$Ra = \frac{\left[\left(mH_3/H_1\right)^2 + \left(nH_3/H_2\right)^2 + q^2\right]^2 \pi^2}{\left(mH_3/H_1\right)^2 + \left(nH_3/H_2\right)^2}. \tag{42}$$

Note that eq. (42) is a general expression for the critical Rayleigh numbers of the 3-D fault zone. These critical Rayleigh numbers describe the onset conditions of the convective flows in the system. Since the linear stability concept is used in the analysis, it is important to find the minimum critical Rayleigh number, which corresponds to the most possible convective flow structure in the system. For the given fault zone configuration shown in Fig. 1, since the lengths of the fault zone in all three directions are finite, we can set $m = n = q = 1$ and allow H_1 to vary in the fault length direction. This means that both the height and the thickness of the fault zone are fixed as constants, but the length of the fault zone can change as a variable of the system. Through selecting the appropriate value of H_1, the minimum critical Rayleigh number of the system can be determined. For this purpose, the critical Rayleigh number for the 3-D convection flow to take place can be expressed as

$$Ra_{\text{critical}}^{\text{3D}} = \frac{\left[\left(H_3/H_1\right)^2 + \left(H_3/H_2\right)^2 + 1\right]^2 \pi^2}{\left(H_3/H_1\right)^2 + \left(H_3/H_2\right)^2}. \tag{43}$$

Differentiating eq. (43) with respect to H_1 yields the following equation:

$$\frac{dRa_{\text{critical}}^{\text{3D}}}{dH_1} = -2\pi^2 \frac{H_3^2\left\{\left[\left(H_3/H_1\right)^2 + \left(H_3/H_2\right)^2\right]^2 - 1\right\}}{H_1^3\left[\left(H_3/H_1\right)^2 + \left(H_3/H_2\right)^2\right]^2} \approx -2\pi^2 \frac{H_3^2}{H_1^3}. \tag{44}$$

Note that eq. (44) is valid when $H_3/H_2 \gg 1$ and $H_1/H_2 \gg 1$, which are true for the fault zone considered in this study. Eq. (44) indicates that the minimum critical Rayleigh number of the system is obtained only when H_1 tends to infinity. In such a case, the wavenumber in the x_1 direction is zero and the convective flow is essentially 2-D convective flow, which is the degenerate case of the 3-D convective flow. We call this kind of convective flow the 2-D slender-circle convective flow with the following minimum critical Rayleigh number:

$$Ra_{\text{critical}}^{\text{2D}} = \frac{\left[1 + \left(H_3/H_2\right)^2\right]^2 \pi^2}{\left(H_3/H_2\right)^2}. \tag{45}$$

Eq. (44) also indicates that when $H_3/H_1 \ll 1$, the critical Rayleigh number of the system changes very slowly so that the differences between the corresponding critical Rayleigh numbers and the minimum critical Rayleigh number of the system are very small. This means that several convective flow structures may have almost the same chance of taking place in the system. Since the 3-D standard convective flow structures are only of interest here, we consider the case of $H_3 = H_1$ and determine the corresponding critical Rayleigh number below. If $H_3 = H_1$, we have the following equation:

$$Ra^{3D}_{critical} = \frac{\left[2 + (H_3/H_2)^2\right]^2 \pi^2}{1 + (H_3/H_2)^2}. \quad (46)$$

It is obvious that the critical Rayleigh number for 3-D standard convective flow to occur is proportional to the ratio of the fault height to thickness.

Clearly, the relative difference between $Ra^{3D}_{critical}$ and $Ra^{2D}_{critical}$ can be expressed from eqs (45) and (46) as follows:

$$\bar{\Delta}_1 = \frac{Ra^{3D}_{critical} - Ra^{2D}_{critical}}{Ra^{2D}_{critical}} = \frac{(H_3/H_2)^4 + (H_3/H_2)^2 - 1}{\left[(H_3/H_2)^2 + 1\right]^3}. \quad (47)$$

Since $H_3/H_2 \gg 1$, eq. (47) can be written approximately as

$$\bar{\Delta}_1 \approx \left(\frac{H_2}{H_3}\right)^2. \quad (48)$$

Eq. (48) indicates that the relative difference between $Ra^{3D}_{critical}$ and $Ra^{2D}_{critical}$ is a second-order small quantity, provided that H_2/H_3 is very small, just as considered in this study. For example, if $H_2/H_3 = 0.01$, the relative difference between $Ra^{3D}_{critical}$ and $Ra^{2D}_{critical}$ is approximately 0.0001, which is indeed a very small number. In this case, $Ra^{3D}_{critical} \approx 98\,716.2$, while $Ra^{2D}_{critical} \approx 98\,726.1$. It is noted that the relative difference between $Ra^{3D}_{critical}$ and $Ra^{2D}_{critical}$ approaches zero as H_2/H_3 tends to zero.

Similarly, for the 3-D finger-like convective structure, the corresponding critical Rayleigh number can be expressed as

$$Ra^{3D\text{-finger}}_{critical} = \frac{\left[m^2 + (H_3/H_2)^2 + 1\right]^2 \pi^2}{m^2 + (H_3/H_2)^2} \quad (m \geq 2). \quad (49)$$

In the case of $m = 3$ and $H_2/H_3 = 0.01$, the corresponding $Ra^{3D-finger}_{critical} \approx 98\,805$. Again, this value is also very close to the minimum critical Rayleigh number of the system, $Ra^{2D}_{critical} \approx 98\,726.1$. This indicates that the 3-D finger-like convective flow can also take place in the 3-D fault zones. As the recent numerical simulation of the convective flow in a vertically oriented geological fault zone has demonstrated, the 3-D finger-like convective flow indeed occurred in the system (Rabinowicz *et al.* 1999).

The possible occurrence of the 3-D finger-like convective flow has a significant geological implication for ore body formation and mineralization within 3-D geological fault zones. Since the down-temperature convective flow may result in mineral precipitation and the up-temperature convective flow may result in mineral dissolution, the periodic mineral zonation can be produced within the 3-D geological fault zones. Such a quasi-periodic distribution of the mineralization phenomenon has been observed in the Yilgarn ore deposits, Western Australia.

It is noted that the following relation exists:

$$k_i^* = k_i H, \quad (50)$$

where k_i is the dimensional wavenumber in the real physical system.

For the 3-D fault zone considered in this study, the dimensional wavenumbers are as follows:

$$k_1 = \frac{m\pi}{H_1}, \quad k_2 = \frac{n\pi}{H_2}, \quad k_3 = \frac{q\pi}{H_3}. \quad (51)$$

Finally, the dimensionless perturbation solutions for pore-fluid velocity, temperature and pressure can be derived and expressed as

$$\hat{u}_1^* = -\frac{k_1^* k_3^* \left(k_1^{*2} + k_2^{*2} + k_3^{*2}\right)}{k_1^{*2} + k_2^{*2}} \sin\left(k_1^* x_1^*\right) \sin\left(k_2^* x_2^*\right) \cos\left(k_3^* x_3^*\right) \quad (52)$$

$$\hat{u}_2^* = \frac{k_2^* k_3^* \left(k_1^{*2} + k_2^{*2} + k_3^{*2}\right)}{k_1^{*2} + k_2^{*2}} \cos\left(k_1^* x_1^*\right) \cos\left(k_2^* x_2^*\right) \cos\left(k_3^* x_3^*\right) \quad (53)$$

$$\hat{u}_3^* = \left(k_1^{*2} + k_2^{*2} + k_3^{*2}\right) \cos\left(k_1^* x_1^*\right) \sin\left(k_2^* x_2^*\right) \sin\left(k_3^* x_3^*\right) \quad (54)$$

$$\hat{T}^* = \cos\left(k_1^* x_1^*\right) \sin\left(k_2^* x_2^*\right) \sin\left(k_3^* x_3^*\right) \quad (55)$$

$$\hat{p}^* = \cos\left(k_1^* x_1^*\right) \sin\left(k_2^* x_2^*\right) f\left(x_3^*\right), \quad (56)$$

where $f(x_3^*)$ can be determined by integrating eq. (34) with respect to x_3^* as follows:

$$f\left(x_3^*\right) = -\frac{Ra - \left(k_1^{*2} + k_2^{*2} + k_3^{*2}\right)}{k_3^*} \cos\left(k_3^* x_3^*\right). \quad (57)$$

4 POSSIBILITY OF CONVECTIVE FLOW IN A GEOLOGICAL FAULT ZONE SYSTEM

In this section, the analytical solution derived in the previous section is used to investigate the possibility of convective flow in geological fault zone systems. With an idealized geological fault zone taken as an illustrative example, the following parameters were used in the following analysis. For the pore fluid, the dynamic viscosity is 10^{-3} N s m^{-2}, the reference density is 1000 kg m^{-3}, the volumetric thermal expansion coefficient is 2.07×10^{-4} (1 K^{-1}), the specific heat is 4185 J (kg K)$^{-1}$ and the thermal conductivity coefficient is 0.6 W (m K)$^{-1}$. For the porous matrix, the porosity is 0.1, the thermal conductivity coefficient is 3.35 W (m K)$^{-1}$, the specific heat is 815 J (kg K)$^{-1}$ and the permeability is 10^{-12} m^2, which is assumed as an effective value for a fractured environment (Berryman & Wang 1995); the height and thickness of the fault are 10 and 0.5 km, respectively; the temperature at the top and bottom is 25 and 225 °C, respectively.

Substituting the related parameters into eq. (14) yields the Rayleigh number for the system:

$$\begin{aligned} Ra &= \frac{(\rho_0 c_p)\rho_0 g \beta \Delta T k_0 H}{\mu \lambda_0^e} \\ &= \frac{1000 \times 4185 \times 1000 \times 9.8 \times 2 \times 10^{-4} \times 200 \times 10^{-12} \times 10^4}{10^{-3} \times 3} \\ &\approx 5380. \end{aligned} \quad (58)$$

The corresponding minimum critical Rayleigh number of the fault zone of infinite length is

$$Ra^{2D}_{critical} = \frac{\left[1 + (H_3/H_2)^2\right]^2 \pi^2}{(H_3/H_2)^2} = \frac{(1 + 20^2)^2 \pi^2}{20^2} \approx 3967.6. \quad (59)$$

The corresponding critical Rayleigh number for the 3-D standard convective flow is

$$Ra^{3D}_{critical} = \frac{\left[2 + (H_3/H_2)^2\right]^2 \pi^2}{1 + (H_3/H_2)^2} = \frac{(2 + 20^2)^2 \pi^2}{1 + 20^2} \approx 3977.5. \quad (60)$$

In the case of $m = 3$, the corresponding critical Rayleigh number for the 3-D convective flow is

$$\begin{aligned} Ra^{3D\text{-finger}}_{critical} &= \frac{\left[m^2 + (H_3/H_2)^2 + 1\right]^2 \pi^2}{m^2 + (H_3/H_2)^2} = \frac{(10 + 20^2)^2 \pi^2}{9 + 20^2} \\ &\approx 4056.5. \end{aligned} \quad (61)$$

Because the above three critical Rayleigh numbers are very close to each other and $Ra > Ra^{3d-finger}_{critical}$, the corresponding three kinds of convective flow may have a similar probability of taking place in the geological fault zone considered here.

Note that the 2-D slender-circle structure of convection cells can only take place when the length of the fault zone is infinite (i.e.

H_1 approaches infinite). This means that no convection cell takes place in the x_1 direction and the 2-D slender-circle flow structure is obtained in the plane perpendicular to the x_1 axis. However, if the length of the fault zone is finite, the corresponding convective flow must be 3-D. Even if the length of the fault zone is infinite, since the minimum critical Rayleigh number of the system (i.e. 3967.6) for the 2-D slender-circle flow structure is so close to the critical Rayleigh number (i.e. 3977.5) for the 3-D standard convective flow structure, the system may have a similar possibility to pick up the 3-D convective flow structure. Since the convection modes are so close for the 3-D convective flow structures, the convective flow may also evolve into a 3-D finger-like structure (e.g. $m \geq 2$). This finding demonstrates the beautiful aspects of the present analytical solution for the convective instability of 3-D geological fault zones, because this analytical solution is valid for any value of the ratio of the fault height to thickness. Using the present analytical solution, the conditions, under which different convective flow structures may occur in the 3-D fault zone, can be easily determined. This is the major advantage of the present analytical solution in dealing with the convective instability of 3-D geological fault zones when they are heated uniformly from below.

Figs 2 and 3 show the theoretical fundamental mode ($m = 1$) and finger-like mode ($m = 3$) for the perturbed pore-fluid velocity

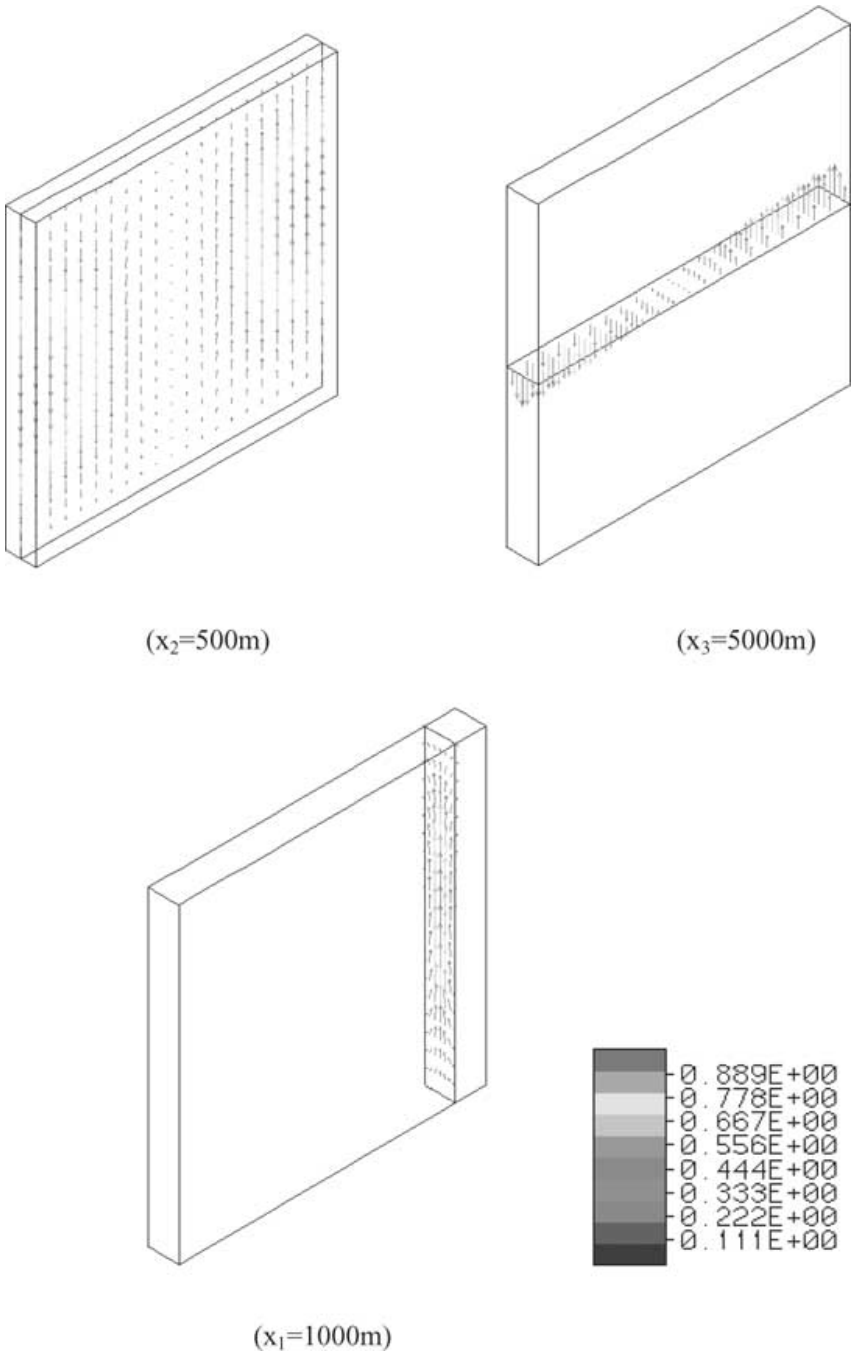

Figure 2. Convective flow mode in the 3-D fault (theoretical fundamental mode).

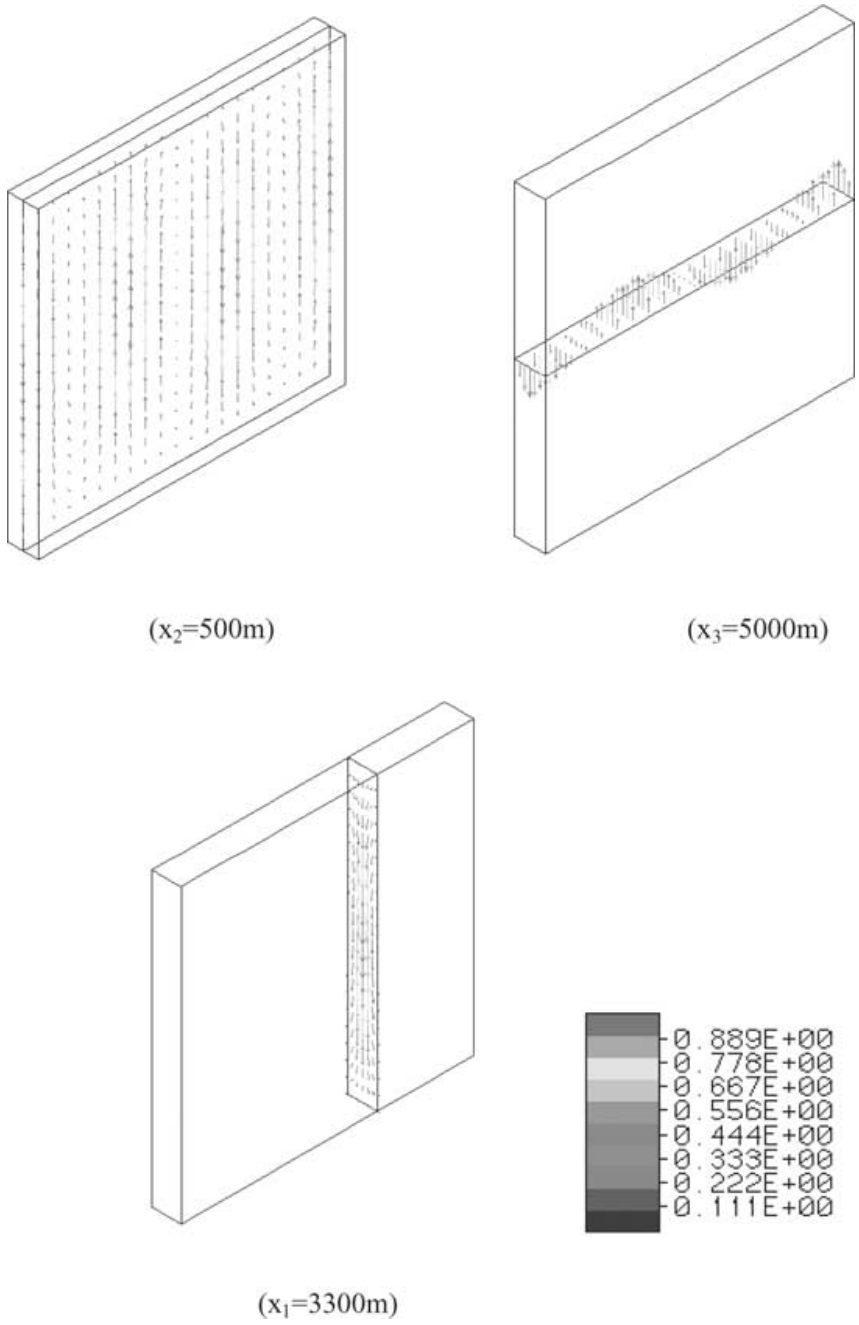

Figure 3. Convective flow mode in the 3-D fault (theoretical finger-like mode).

on three particular cross-sections in a pore-fluid saturated geological fault zone. The length and height of the fault zone are 10 km, while the thickness of the fault zone is 1 km. It is obvious that the convective pore-fluid flow takes place strongly in the vertical direction. Indeed, the horizontal pore-fluid velocity is negligible on both the sidewalls (i.e. $x_2 = 0$ and H_2) of the fault zone, although the hydrostatic pore-fluid pressure gradient condition is used in the analysis. In the case of the finger-like mode, the pore-fluid flow channeling can be clearly observed. This pore-fluid flow channeling phenomenon can significantly influence the ore body formation and mineralization patterns within the geological fault zone.

5 CONCLUSIONS

Exact analytical solutions to the critical Rayleigh numbers of different convective flow structures have been derived for 3-D fluid-saturated geological fault zones when they are heated uniformly from below. Using the corresponding critical Rayleigh numbers, three interesting convective flow structures can be identified in a geological fault zone system. If the length of the fault zone is infinite, the critical Rayleigh number has a minimum value, which corresponds to the 2-D slender-circle convective flow structure with the critical Rayleigh number expressed in eq. (45). This slender-circle

convective flow structure takes place in the plane perpendicular to the x_1 axis.

If the length of the fault zone is finite, the corresponding convective flow must be 3-D. Even if the length of the fault zone is infinite, since the minimum critical Rayleigh numbers of the system are very close to each other, the 3-D convective flow may have a similar possibility of taking place in the system, especially when the fault thickness to height ratio is very small. For the 3-D standard convective flow structure, the corresponding critical Rayleigh number is expressed in eq. (46).

For the 3-D finger-like convective structure, the corresponding critical Rayleigh number can be expressed in eq. (49).

ACKNOWLEDGMENTS

The authors are very grateful to the anonymous referees for their valuable comments on an early draft of this paper. They also express thanks for the financial support from the CSIRO/CAS exchange programme, the CAS programme (programme no KZCX2-113) and the Predictive Mineral Discovery Coorperative Research Centre.

REFERENCES

Beck, J.L., 1972. Convection in a box of porous material saturated with fluid, *Phys. Fluids,* **15,** 1377–1383.

Berryman, J.G. & Wang, H.F., 1995. The elastic coefficients of double-porosity models for fluid transport in jointed rock, *J. geophys. Res.,* **100,** 24 611–24 627.

Horton, C.W. & Rogers, F.T., 1945. Convection currents in a porous medium, *J. Appl. Phys.,* **16,** 367–370.

Kassoy, D.R. & Cotte, B., 1985. The effects of sidewall heat loss on convection in a saturated porous vertical slab, *J. Fluid Mech.,* **152,** 361–378.

Lapwood, E.R., 1948. Convection of a fluid in a porous medium, *Proc. Camb. Phil. Soc.,* **44,** 508–521.

Lowell, R.P. & Shyu, C.T., 1978. On the onset of convection in a water-saturated porous box: effect of conducting walls, *Lett. Heat Mass Transfer,* **5,** 371–378.

McTigue, D.F., 1986. Thermoelastic response of fluid-saturated porous rock, *J. geophys. Res.,* **91,** 29 533–29 542.

Murphy, H.D., 1979. Convective instabilities in vertical fractures and faults, *J. geoghys. Res.,* **84,** 6121–6130.

Nield, D.A. & Bejan, A., 1992. *Convection in Porous Media,* Springer, New York.

Phillips, O.M., 1991. *Flow and Reactions in Permeable Rocks,* Cambridge University Press, Cambridge.

Rabinowicz, M., Sempere, J.C. & Genthon, P., 1999. Thermal convection in a vertical permeable slot: implications for hydrothermal circulation along mid-ocean ridges, *J. geophys. Res.,* **104,** 29 275–29 292.

Rice, J.R. & Cleary, M.P., 1976. Some basic stress diffusion solutions for fluid-saturated elastic porous media with compressible constituents, *Rev. Geophys. Space Phys.,* **14,** 227–241.

Zebib, A. & Kassoy, D.R., 1977. Onset of natural convection in a box of water-saturated porous media with large temperature variation, *Phys. Fluids,* **20,** 4–9.

Zhao, C., Mühlhaus, H.B. & Hobbs, B.E., 1997. Finite element analysis of steady-state natural convection problems in fluid-saturated porous media heated from below, *Int. J. Num. Analy. Meth. Geomech.,* **21,** 863–881.

Zhao, C., Hobbs, B.E. & Mühlhaus, H.B., 1998a. Analysis of pore-fluid pressure gradient and effective vertical-stress gradient distribution in layered hydrodynamic systems, *Geophys. J. Int.,* **134,** 519–526.

Zhao, C., Hobbs, B.E. & Mühlhaus, H.B., 1998b. Finite element modelling of temperature gradient driven rock alteration and mineralization in porous rock masses, *Compu. Meth. Appl. Mech. Eng.,* **165,** 175–187.

Zhao, C., Hobbs, B.E. & Mühlhaus, H.B., 1999a. Theoretical and numerical analyses of convective instability in porous media with upward throughflow, *Int. J. Num. Analy. Meth. Geomech.,* **23,** 629–646.

Zhao, C., Hobbs, B.E. & Mühlhaus, H.B., 1999b. Finite element modelling of reactive mass transport problems in fluid-saturated porous media, *Commun. Numer. Methods Eng.,* **15,** 501–513.

Zhao, C., Hobbs, B.E., Mühlhaus, H.B. & Ord, A., 1999c. Finite element analysis of pore-fluid flow patterns near geological lenses in hydrodynamic and hydrothermal systems, *Geophys. J. Int.,* **138,** 146–158.

Zhao, C., Hobbs, B.E., Mühlhaus, H.B., Ord, A. & Lin, G., 2000a. Numerical modelling of double diffusion driven reactive flow transport in deformable fluid-saturated porous media with particular consideration of temperature-dependent chemical reaction rates, *Int. J. Computer-aided Eng. Software: Eng. Comput.,* **17,** 367–385.

Zhao, C., Hobbs, B.E., Mühlhaus, H.B. & Ord, A., 2000b. Finite element modelling of dissipative structures for nonequilibrium chemical reactions in fluid-saturated porous media, *Comp. Meth. Appl. Mech. Eng.,* **184,** 1–14.

Zhao, C., Hobbs, B.E., Mühlhaus, H.B., Ord, A. & Lin, G., 2001a. Finite element modelling of 3-D convection problems in fluid-saturated porous media heated from below, *Commun. Numer. Methods Eng.,* **17,** 101–114.

Zhao, C., Hobbs, B.E., Walshe, J.L., Mühlhaus, H.B. & Ord, A., 2001b. Finite element modeling of fluid-rock interaction problems in pore-fluid saturated hydrothermal/sedimentary basins, *Comp. Methods Appl. Mech. Eng.,* **190,** 2277–2293.